environmental microbiology

Environmental Microbiology (2012) doi:10.1111/1462-2920.12038

In situ chemistry and microbial community compositions in five deep-sea hydrothermal fluid samples from Irina II in the Logatchev field

Mirjam Perner,[1]* Giorgio Gonnella,[2] Stephane Hourdez,[3,4] Stefanie Böhnke,[1] Stefan Kurtz[2] and Peter Girguis[5]

[1]*Molecular Biology of Microbial Consortia, University of Hamburg, Biocenter Klein Flottbek, Ohnhorststr. 18, 22609 Hamburg, Germany.*

[2]*Center for Bioinformatics, University of Hamburg, Bundesstrasse 43, 20146 Hamburg, Germany.*

[3]*Genetics of Adaptation to Extreme Environments Group, UMR7144, CNRS, Station Biologique de Roscoff, 29680 Roscoff, France.*

[4]*Genetics of Adaptation to Extreme Environments Group, UMR7144, Université Pierre et Marie Curie, Station Biologique de Roscoff, 29680 Roscoff, France.*

[5]*Organismic and Evolutionary Biology, Harvard University, Cambridge, MA 02138, USA.*

Summary

We present data on the co-registered geochemistry (*in situ* mass spectrometry) and microbiology (pyrosequencing of 16S rRNA genes; V1, V2, V3 regions) in five fluid samples from Irina II in the Logatchev hydrothermal field. Two samples were collected over 24 min from the same spot and further three samples were from spatially distinct locations (20 cm, 3 m and the overlaying plume). Four low-temperature hydrothermal fluids from the Irina II are composed of the same core bacterial community, namely specific *Gammaproteobacteria* and *Epsilonproteobacteria*, which, however, differs in the relative abundance. The microbial composition of the fifth sample (plume) is considerably different. Although a significant correlation between sulfide enrichment and proportions of *Sulfurovum* (*Epsilonproteobacteria*) was found, no other significant linkages between abiotic factors, i.e. temperature, hydrogen, methane, sulfide and oxygen, and bacterial lineages were evident. Intriguingly, bacterial community compositions of some time series samples from the same spot were significantly more similar to a sample collected 20 cm away than to each other. Although this finding is based on three single samples only, it provides first hints that single hydrothermal fluid samples collected on a small spatial scale may also reflect unrecognized temporal variability. However, further studies are required to support this hypothesis.

Introduction

Hydrothermal vents are hallmarked by steep thermal and chemical gradients, which form as ascending hot, reduced hydrothermal fluids mix with entrained cold, oxygenated ambient seawater. Owing to these mixing processes, inorganic reduced energy-rich electron donors and oxidized electron acceptors are both present. Their availability is expected to largely govern microbial community composition (Perner *et al*., 2010; 2011) and, since these substrates can fuel chemosynthetic metabolism, affect microbial biomass production as well (McCollom, 2007). The emitted hydrothermal fluids and the entrained microorganisms can provide us with an insight into the physicochemical conditions of the subsurface pathways the fluids flow through on the way to the surface.

Chemical signatures of hydrothermal fluids are known to fluctuate over space and time (e.g. LeBris *et al*., 2006; Rogers *et al*., 2007; Zielinski *et al*., 2011), and appear to have an impact on the local microbial diversity (Perner *et al*., 2010; 2011). As such, it is not surprising to find small-scale (few centimetres to metres) (Nakagawa *et al*., 2005) and large-scale (Perner *et al*., 2007; Huber *et al*., 2010) dynamics in microbial populations. However, while large-scale intra- and inter-field variability has been studied several times (Perner *et al*., 2007; Davis and Moyer, 2008; Nanoura and Takai, 2009; Huber *et al*., 2010; Flores *et al*., 2012), few studies have examined genuine small-scale (Nakagawa *et al*., 2005) and short-term temporal (Perner *et al*., 2009) microbial dynamics in hydrothermally influenced provinces. Understanding the variability in hydrothermal vent systems – and the scale at which these variations occur – remains challenging to date. So far, temporal and/or spatial chemical and microbial changes have been ascribed to the type of host rock, degrees of subsurface dilution, precipitation processes,

Received 7 June, 2012; accepted 29 October, 2012. *For correspondence. E-mail mirjam.perner@uni-hamburg.de; Tel. (+49) 40 42816 444; Fax (+49) 40 42816 459.

microbial activities in the subsurface, tidal and bottom currents, seismic events and altered fluid pathways (Perner *et al*., 2009; and references therein).

To better understand the relationships between microbial ecology (composition, structure, density), physiology (energy metabolism) and geochemistry, recent studies have used high-throughput sequencing technologies and sometimes geochemical measurements (Rocap *et al*., 2003; DeLong *et al*., 2006; Huber *et al*., 2010; Flores *et al*., 2012). High-throughput sequencing allows unprecedented sampling depth and hence provides new insights into microbial communities (e.g. Sogin *et al*., 2006). Sequencing of selected phylogenetic markers like 16S rRNA genes can uncover yet unexplored diversity, revealing biological patterns which can be allocated to specific habitat characteristics (Brazelton *et al*., 2010; Huber *et al*., 2010). Many such studies have focused on marine microbial ecology, although predominantly in the water column (e.g. Rocap *et al*., 2003; DeLong *et al*., 2006). To date, far fewer studies have employed high-throughput sequencing technologies and simultaneously registered geochemical measurements in marine benthic environments, including vents (Huber *et al*., 2007; 2010; Brazelton *et al*., 2010).

Applied at vents, this approach would allow examining the relationship between geochemistry and microbial community composition at temporal and spatial scales appropriate to the environment. As mentioned, previous studies have focused largely on this relationship at the regional scale, which can address questions about biogeography. To better understand how microbial community composition relates to temporal and spatial variations in chemistry at the mesoscale (tens of centimetres, over minutes to hours), we conducted a series of experiments to examine short-term temporal and small-scale spatial dynamics of hydrothermally influenced fluids and bacterial community composition using *in situ* mass spectrometry (ISMS) and pyrosequencing of the 16S rRNA genes – pyrotag sequencing including regions V1, V2 and V3. We collected four low-temperature hydrothermal fluid samples (samples A–D) and one plume water sample (sample E) from the ultramafic-hosted Logatchev field. Samples A through D were recovered from a connected mussel field bordering the main structure Irina II. Two samples (A and B) were collected over 24 min from the same location to investigate short-term temporal variability. Samples C and D were recovered from 20 cm and roughly 3 m, respectively, from the site where samples A and B were retrieved. Sample E originates from the hydrothermal plume at 175 m above Irina II. With these co-registered geochemical and microbial data, we can, for the first time, interrogate *in situ* chemistry and microbial dynamics and their interconnections at a deep-sea hydrothermal vent.

Results and discussion

To better constrain the significance of any differences among the samples, we worked to characterize the bias associated with our applied methodology. We performed three 10-cycle PCRs of 16S rRNA genes (e.g. 1A, 2A, 3A) for each of the five samples (samples A–E) to gain sufficient material for sequencing. Each of these PCR amplicons was then divided into three subsamples (e.g. 1A1, 1A2, 1A3) and finally pyrosequenced. Three runs were performed on equally treated subsamples (for nomenclature of subsamples, see Table S1). With respect to technical biases we found small variations between the different sequencing runs, but not between the above mentioned PCRs of one sample (Figs S1 and S2). While the qualitative diversity means appeared to be generally preserved in our subsamples, the quantitative measure uncovered minimal population skewing within the same sample with respect to different sequencing runs (Fig. S2). Since our communities are distinctly different, this bias does not affect our interpretation. Such skewing, however, may lead to misinterpretation of data when investigating minor variations between microbial communities sequenced in different runs and is thus important to consider.

Time series of hydrothermal fluid samples

The *in situ* fluid chemistry and associated bacterial community composition was monitored over a time period of 24 min in hydrothermal fluids emitted from the same point (denoted samples A and B). During this time the sampling device was not moved from the location and thus any detected changes are related to intrinsic effects in the system. Within the 24 min the temperature increased from around 6.4°C to a maximum of 11°C (Fig. 1A). There were also significant increases in hydrogen (from 162 μM to max. 327 μM) and methane (from 47 μM to 102 μM) (Fig. 1B) and a small decrease in oxygen (235 μM to 208 μM) (P-value < 0.001 for all gases) (Fig. 1A) suggesting an elevated hydrothermal endmember contribution and thus more reducing conditions. However, magnesium concentrations remained fairly constant around 51 to 52 mM (Fig. 1A). During sampling, the cell numbers decreased by 60% from 5.1×10^5 cells ml^{-1} to 2.0×10^5 cells ml^{-1} (Fig. S3), while diversity increased (Shannon diversity indices: sample A 3.3 ± 0.1 and sample B 5.3 ± 0.2) (Fig. S4). Both cell numbers and diversity indices are in the magnitude of what is commonly found in hydrothermal venting regimes (Nakagawa *et al*., 2005; Perner *et al*., 2009). The communities from samples A (first 10 min) and B (subsequent 14 min) were significantly different (P-value < 0.05) and a shift in the bacterial community within the 24 min was clearly evident (Fig. 2). During the first 10 min of

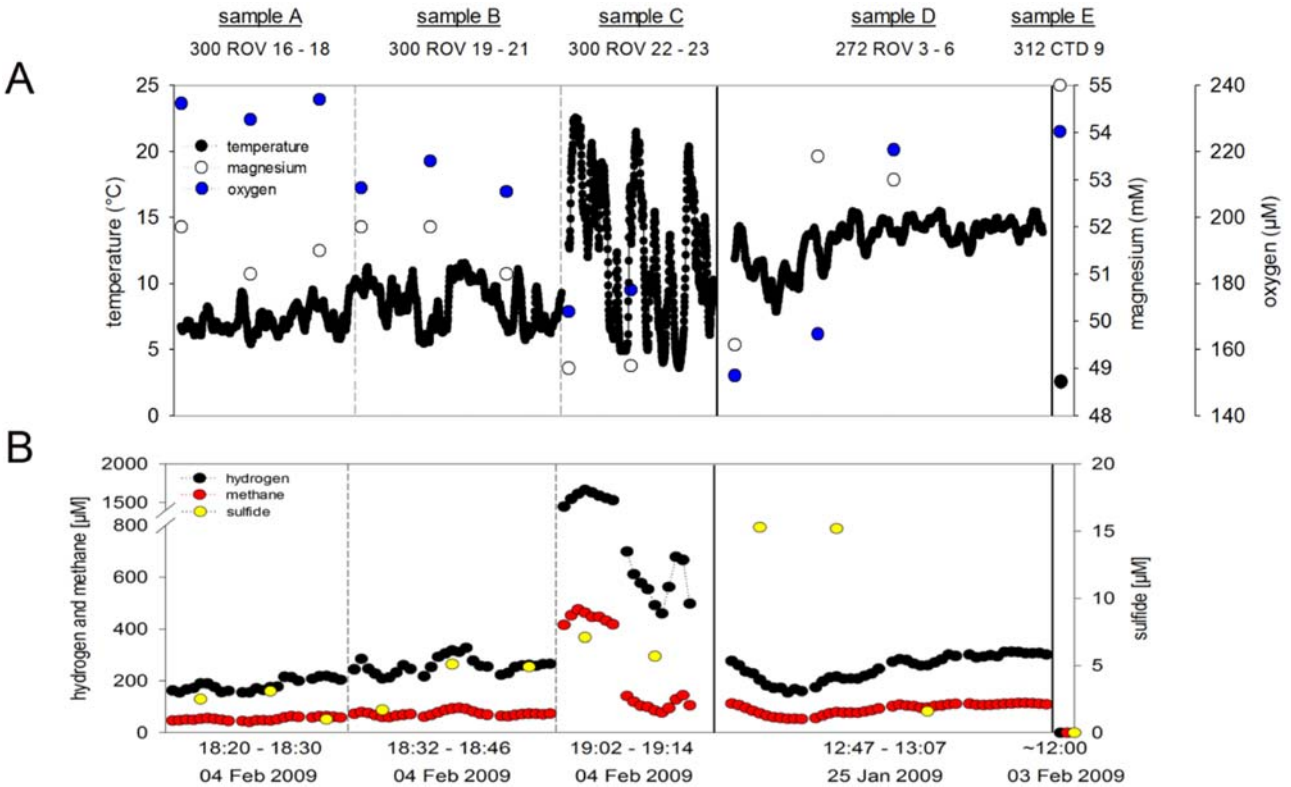

Fig. 1. A. Temperature, oxygen and magnesium concentrations for Irina II hydrothermally influenced fluids.
B. Hydrogen, methane and sulfide concentrations for Irina II hydrothermally influenced fluids. Hydrogen and methane concentrations were measured *in situ* by the ISMS unit. Temperature was monitored *in situ* with the KIPS. Oxygen, magnesium and sulfide concentrations were measured *ex situ*. For the plume samples hydrogen and methane concentrations were determined *ex situ*, too. The sampling times are in UTC (universal time code).

sampling (sample A) the majority of 16S rRNA genes were affiliated with *Gammaproteobacteria* of the genera *Alcanivorax* and *Marinobacter* (65–74%) and only few *Epsilonproteobacteria* (17–24%) were recognized (Fig. 2A). For the 14 min thereafter (sample B) the inverse was the case: *Epsilonproteobacteria* 61–71% and *Gammaproteobacteria* 16–27% (Fig. 2A). Additionally, representatives of the thermophilic *Aquificae* increased during the sampling. The changes in chemistry, from more oxidizing to more reducing conditions, reflect the potential physiologies of the bacteria found in the samples. *Alcanivorax* and *Marinobacter* are associated with moderate temperatures and oxygenated conditions (Gonzalesz and Whitman, 2006). In contrast, the *Epsilonproteobacteria* enriched in sample B, namely thermophilic *Caminibacter*, and mesophilic *Sulfurovum*, *Arcobacter* and other *Campylobacterales*, are associated with more reducing conditions, where levels of sulfide and hydrogen (that serve as electron donor) are elevated (Campbell *et al*., 2006). Particularly, the increased representation of thermophilic, anaerobic or microaerobic, hydrogen-oxidizing *Caminibacter* and *Aquificae* species coincides with the elevated hydrogen concentrations.

Temporal dynamics have been attributed to a broad range of various effects including tidal currents and local bottom currents, seismic events, precipitation processes, different extents of subsurface dilution, alterations in fluid flow pathways, progressing of vent maturity, microbial activities and biological interactions (Perner *et al*., 2009; and references therein). Yet, we suggest that major changes in currents, seismic events or gross changes in vent geochemistry cannot explain our observed differences over the 24 min of sampling because the time scales over which these changes are manifest are too short. Our measured temperature and oxygen concentrations compare to those previously determined at Irina II (Zielinski *et al*., 2011). These data revealed temporal variations in physicochemical conditions (Fig. 1) that are consistent with previously observed highly dynamic changes over short time frames at Irina II (Zielinski *et al*., 2011). This phenomenon has been observed at other vent locations as well (LeBris *et al*., 2006). Nevertheless, besides the data presented here (Fig. 2), to our knowledge, only one other study has investigated and reported changes in vent microbial populations on comparably short time scales (in their case 50 min) (Perner *et al*.,

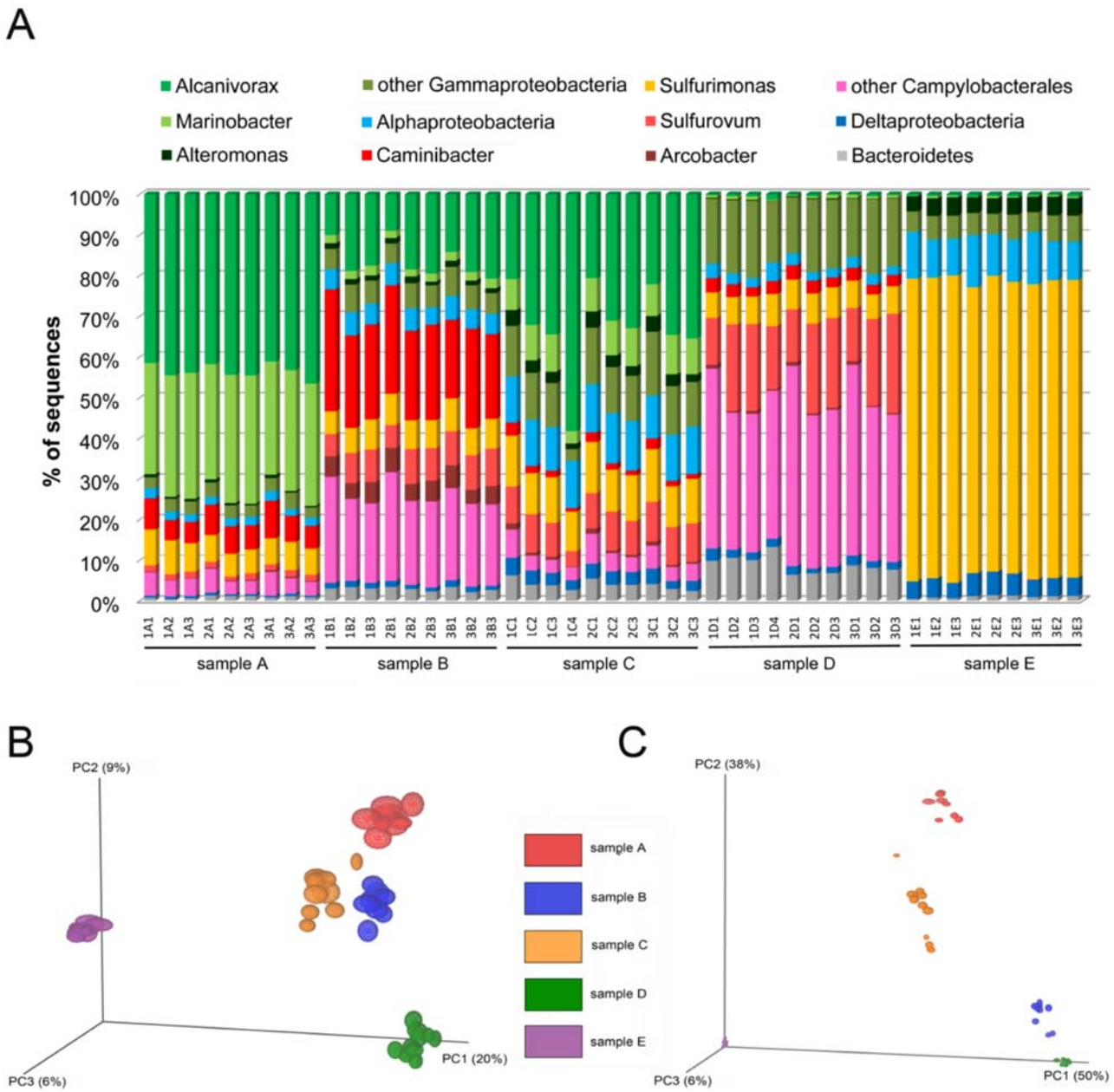

Fig. 2. A. Proportions of bacteria recognized in the three subsamples of the three different PCRs from the four sites and five samples (samples A–E).
B and C. PCoA performed on subsamples from five hydrothermally influenced environments around Irina II using Qiime (Caporaso *et al.*, 2010a). (B) Unweighted and (C) weighted normalized algorithms were used. The dots corresponding to the different bacterial communities are colour-coded according to the different sampling sites: sample A is red, sample B is blue, sample C is orange, sample D is green and sample E is purple. The spheres around the points mark the interquartile ranges (jackknifing support). The first three principal coordinates (PC1, PC2 and PC3) for the subsamples of the five environments are plotted. The axes are labelled by the percentage variation explained by the PCs.

2009). In the latter study, thermodynamic models predicted that predominant energy metabolisms likely changed during the 50 min of sampling (Perner *et al.*, 2009), and the data in the current study are consistent with that hypothesis. In a previous study at the Irina II habitat, physicochemical fluid variability has, among other possibilities, been attributed to mussel colonization which was hypothesized to cause diversion of fluid flow and influence the degree of oxygenated, ambient seawater mixed with the reduced fluids (Zielinski *et al.*, 2011). In the current study, we collected our fluid samples down among the mussels, and immediately above the zone of emission. In light of our mode of sampling, as well as the temperature data (which suggest a lower representation

of ambient seawater when compared with the fluids above the mussels), we suggest that the impact of the mussels is modest. Rather, we posit that the observed changes between the emanated fluids reflect finer-scale alterations in the subsurface flow regime, which influence the proportion and representation of vent and seawater-derived constituents. The availability of these abiotic properties, in turn, have been shown to govern microbial community compositions (e.g. Flores *et al*., 2011; Perner *et al*., 2011). Thus, we propose that the shifts in the microbial population in the emanated fluids can be explained by fluid entrainment of microbes from thermally and chemically heterogenous subsurface habitats along the fluid flow pathways.

Spatially divergent hydrothermal fluid samples

Differences in the community compositions on a small spatial scale (few centimetres to metres) have been found for distinct hydrothermal venting sites (e.g. Nakagawa *et al*., 2005; Davis and Moyer, 2008; Huber *et al*., 2010). For some locations the small spatial microbial heterogeneity has been attributed to the chemistry and temperature prevailing in the habitat (Davis and Moyer, 2008). The bacterial communities from samples A, B (short-term time series data collected from the same spot) and C (collected within a 20 cm radius) were more similar than populations of the more distantly collected samples D (roughly 3 m away) and E (plume waters 175 m above ground) (Figs 2B and S1A, unweighted algorithm). Remarkably, when considering abundance information, the bacterial population of sample C, collected 20 cm from samples A and B, resembles sample A more in its community composition than samples A and B resemble each other (Figs 2C and S1B). Thus, it appears that fluids with similar microbial communities can emit at different locations – on a small spatial scale – and different population compositions can emanate with fluids at the same point of venting on the time scale of minutes. Consequently, the variability observed herein argues for highly dynamic conditions along the fluid pathways, supportive of heterogenous communities, and likely entails variation in metabolic activity.

To identify the possible abiotic parameters responsible for the variations between the bacterial communities, we took co-registered measurements of the local *in situ* chemistry alongside the collection of hydrothermal fluid samples at all four sites. The measured *in situ* chemistry at site C was significantly different to the chemistry of the other low-temperature Irina II samples A, B and D (P-value < 0.05) (Fig. 1). The microbial communities from sample C were also significantly different from those of sample B (P-value < 0.001) and sample D (P-value < 0.01, normalized weighted UniFrac significance). At site C, maximum *in situ* hydrogen and methane concentrations reached 1666 μM and 486 μM, respectively, oxygen and magnesium decreased to 171 μM and 49 mM, respectively, and temperatures reached a maximum of 24°C (Fig. 1). The elevated values indicate an increased endmember contribution, which is consistent with a greater contribution of vent-derived fluids in the subsurface through which the fluids represented by sample C pass. However, this hypothesis is not supported by the microbial community representation, since thermophilic representatives like *Caminibacter* or *Aquificae*, detected in sample B, were hardly present in sample C (Fig. 2A). Instead, in the latter, the majority of bacteria were affiliated to mesophilic *Gammaproteobacteria*, i.e. *Thiomicrospira*, *Alcanivorax*, *Marinobacter* and *Alteromonas*. Mesophilic *Epsilonproteobacteria*, namely *Sulfurovum*, *Sulfurimonas* and some *Campylobacterales*, also made up a considerable proportion of the bacterial community (Fig. 2A). Besides the *Campylobacterales*, which may be involved in hydrogen cycling (Perner *et al*., 2011), the other recognized *Epsilonproteobacteria* can be linked with both sulfur and hydrogen metabolisms (Campbell *et al*., 2006; Nakagawa *et al*., 2007). Temperatures at the exit point where fluids from sample C emit (24°C) are higher than those at the other investigated Irina II sites. However, based on the physiology of the identified fluid microbes, it appears that the sample C fluids flow through pathways in the subsurface with a lower temperature than pathways through which the samples A and B fluids pass, possibly indicating subsurface fluid dilution with deep-sea water for these two samples shortly before exiting the seafloor.

Although hydrogen and methane concentrations at site D are comparable with those in samples A and B (hydrogen 170 μM to 303 μM and methane 50 μM to 111 μM), measured temperatures are higher (16°C), and oxygen at the site reached a record low of 152 μM but then climbed back up to 221 μM (Fig. 1). In contrast to the other sites, sulfide concentrations considerably increased from 1–6 μM to a maximum of 15 μM in sample D (Fig. 1B), which is comparable with previous measurements of sulfide concentrations at Irina II (Zielinski *et al*., 2011). Cell numbers and the diversity index for sample D resembled those of samples B and C (Figs S3 and S4). *Epsilonproteobacteria* were highly enriched at site D and were mostly affiliated with mesophilic *Sulfurovum*, *Sulfurospirillum*, *Sulfurimonas* and *Campylobacterales* (Fig. 2A). According to the unweighted algorithm, the microbial community from D was distinctly different to those in samples A, B and C from Irina II (Fig. 2B). This may be a consequence of the distance to the other sites (roughly 3 m), the closer vicinity to the actual main chimney structure and/or the elevated sulfide concentrations.

As expected, the chemical signature from the plume sample E was significantly different to that of all other low-temperature Irina II diffuse fluids, most likely explaining the significant changes (*P*-value = 0.001–0.01) in the microbial community composition, when compared with samples A, B, C and D (Fig. 2). Hydrogen (14 nM) and methane concentrations (10 nM) were extremely low, sulfide was below the detection limit and oxygen reached the values of the ambient seawater (226 ± 40 μM). Cell counts in the plume dropped to 10% of those in sample A or 20–26% of the counts in samples B, C and D (Fig. S3), and were slightly lower than in other plume samples (Nakagawa *et al*., 2005). The bacterial diversity was even lower than in sample A (Fig. S4). *Sulfurimonas* relatives clearly prevailed the bacterial domain of the plume waters (Fig. 2A). Besides *Sulfurimonas*' ability to grow chemolithoautotrophically, its metabolic versatility (use of various electron donors, electron acceptors and organic carbon sources), oxygen tolerance and environmental sensing systems (Campbell *et al*., 2006; Grote *et al*., 2012) may be its keys to success in this plume water sample. Predominance of a few phylotypes, for example *Epsilonproteobacteria*, has been observed in hydrothermal plumes before (Sunamura *et al*., 2004).

(A)biotic interconnections

In the four tested samples from low-temperature diffuse fluids the same core bacterial community was present, consisting of *Gammaproteobacteria* (*Marinobacter*, *Alcanivorax* and *Thiomicrospira*) and *Epsilonproteobacteria* (*Caminibacter*, *Sulfurimonas*, *Sulfurovum* and *Campylobacterales*) (Fig. 2A). Differences between the populations of the distinct samples are visible in the relative proportions of the core genera and orders. However, only few significant correlations are evident here. There is a significant correlation (*P*-value < 0.05) between the presence of *Marinobacter* and *Alcanivorax* on one side and the abundance of *Sulfurovum* and *Campylobacterales* on the other side. This suggests that these couples may colonize similar habitats or have syntrophic relationships. There are other significant correlations (*P*-value < 0.01) between increased hydrogen and elevated methane concentrations, which in turn correlate with reduced magnesium, or increased temperature and reduced oxygen concentrations. These abiotic–abiotic linkages can be explained by the degree of admixed oxygenated ambient seawater affecting temperature, magnesium, oxygen, hydrogen and methane concentrations. The only abiotic feature significantly correlating with the presence of a bacterial group was the interrelationship between elevated sulfide concentrations and *Sulfurovum* enrichment (*P*-value < 0.01).

Conclusion

When assessing the microbial community on a temporal (two samples collected over 24 min) and a spatial scale (single samples from four locations) a core bacterial community appears to govern the tested Irina II diffuse fluid emissions. Besides the plume sample with distinctly different abiotic conditions to the low-temperature hydrothermal fluids, all other samples have *Gammaproteobacteria* associated with *Marinobacter*, *Alcanivorax* and *Thiomicrospira*, as well as *Epsilonproteobacteria* affiliated with *Caminibacter*, *Sulfurimonas*, *Sulfurovum* and *Campylobacterales* (Fig. 2A). The changes observed between communities collected at the different time points from the same spot and from different locations can mainly be attributed to shifts in the relative abundance of these core bacterial lineages. The differences in the emanated populations may relate to heterogenous conditions in the subsurface along the fluid pathways. However, besides a significant correlation between sulfide enrichment and proportions of *Sulfurovum* (*Epsilonproteobacteria*), no other significant linkages between abiotic factors (temperature, hydrogen, methane, sulfide and oxygen) and bacteria were discerned. This is surprising since in the past interconnections between fluid chemical properties and microbial compositions have been established (e.g. Perner *et al*., 2010; 2011; Flores *et al*., 2011). The lack of further correlations between the microbial community composition and geochemistry may be related to differences in the temporal scales of geochemical sampling. Indeed, the temporal resolution of the temperature and chemistry via the Kieler Pump system (KIPS) and the mass spectrometer, respectively, is on the scale of seconds to tens of seconds; the resolution of the microbial community is much lower and is integrated over several minutes to the limitations of existing apparatus. Hence, if collecting samples for analyses of microbial community compositions was possible on the scale of seconds, the highly variable chemistry may be better linkable to the biology. Alternatively, the level of the phylogenetic resolution may be too broad for detecting correlations or 16S rRNA gene phylogenetic analysis may not be able to reveal functional responses of the microbial community to changes in fluid chemistry.

Interestingly, one of the bacterial populations from the two time series samples was in fact more similar to the integrated community sampled 20 cm away than to the population in the sample collected from the same location in the following 14 min. Although replicates are missing, we posit from this data set that small-scale spatial diversity observed within a vent location may also arise – to some yet undetermined degree – from unrecognized temporal diversity changes. Further studies will be required to confirm this hypothesis.

Experimental procedures

Site descriptions and sample collection

Five hydrothermally influenced fluid samples (samples A, B, C, D and E) were collected from the Logatchev field at 14°45′N located at a water depth around 3000 m along the Mid-Atlantic Ridge (MAR) (Perner *et al*., 2007). Hydrothermal fluids were retrieved during dives with the remotely operated vehicle Kiel ROV 6000 (IFM-GEOMAR, Kiel) during the cruise HYDROMAR VI (January/February 2009) with the RV Maria S. Merian. Detailed sampling procedures are described elsewhere (Perner *et al*., 2009). Irina II is the main chimney structure in the Logatchev field. It is surrounded by a *Bathymodiolus* mussel patch, which is colonized by crabs, brittle stars, snails and isolated shrimps. Samples A to D were retrieved from locations where low-temperature hydrothermal fluids emitted from one connected mussel patch by positioning the nozzle of the fluid sampling system deep between the mussels, but not in contact with the substrate. While samples A and B were taken exactly at the same location at different time points (sample A on 4 February 2009, 18:20–18:30 UTC and sample B on 4 February 2009, 18:32–18:46 UTC) and thus represent temporal dynamics, sample C was collected (4 February 2009, 19:02–19:14 UTC) roughly 20 cm away from samples A and B and represents short-range spatial variation. Samples A, B and C were taken roughly 3 m away from the main Irina II structure, and sample D (25 January 2009, 12:47–13:07 UTC) was retrieved just at Irina II's base. Sample E was taken from the hydrothermal plume 175 m above the ground of Irina II (3 February 2009, around 12:00 UTC).

Fluid chemistry

We used the same methods for ISMS as in Wankel and colleagues (2011) to measure hydrogen and methane concentrations in the field. Briefly, the ISMS unit was configured to sample fluids at temperatures up to 350°C by drawing sample through a titanium heat exchanger prior to passing it by the membrane. A Seabird CTD pump is used to move sample at a rate of ~ 50 ml min^{-1}. During these deployments, Teflon AF™ backed by an integrated polyvinylidene fluoride sheet (Random Technologies, San Francisco, CA, USA) was used *in lieu* of a polydimethylsulfidone (PDMS) membrane, due to its consistent performance over a wide range of hydrostatic pressures. Power (24VDC) and communications (RS-232) to the instrument were supplied from the submersible via dielectric oil-compensated junction box and underwater connectors (SubConn, Burwell, NE, USA). Serial communications with the turbo pump (which provided feedback on vacuum status and chamber temperature, etc.) and the RGA mass analyser enabled real time monitoring of instrument response directly from within the control room on board. Using water ion intensity as a proxy for temperature and the associated changes in analyte permeability, thermal artefacts – if any – are removed from the true signal. Once normalized, signal intensity is used to determine concentrations by comparison with laboratory-generated data for each analyte (see Wankel *et al*., 2011). Because the use of Teflon AF™ can prevent robust oxygen and sulfide quantification, oxygen and sulfide were measured directly on board (*ex situ*). For these latter molecules, routine procedures were applied: Winkler titration for dissolved oxygen (Carpenter, 1965) and photometry of dissolved sulfide following the methylene blue method (Cline, 1969). Measurements of sulfide concentrations are at the courtesy of H. Strauss (Westfälische Wilhelms-Universität Münster, Germany). Temperature was measured *in situ* with the KIPS as described previously (Perner *et al*., 2009). Magnesium in hydrothermal fluids was determined in the home laboratory by inductively coupled plasma-optical emission spectrometry using a CIROS SOP instrument (Spectro, Germany). Temperature and magnesium are at the courtesy of D. Garbe-Schönberg (Christian-Albrechts-Universität, Kiel, Germany). Hydrogen and methane in the plume waters were analysed on board by a gas chromatograph-equipped pulsed discharge detector (PDD) and by applying a purge and trap technique respectively (cf. Perner *et al*., 2007). *Ex situ* hydrogen and methane concentrations of the plume are at the courtesy of R. Seifert (University Hamburg). The significance of the chemical differences between distinct samples and the correlations between abiotic properties and microbial community compositions were determined by the Student's *t*-test and by Pearson's correlation (SPSS version 16.0; SPSS, Chicago, IL, USA).

Cell counts, DNA extraction and amplification

Procedures for cell counts of each sample were followed as previously described (Perner *et al*., 2010). For DNA extraction of each of the samples A, B, C and D, 450 ml of hydrothermal fluids and, for sample E, 1 l of plume waters were concentrated on polycarbonate filters (type: GTTP, pore size 0.2 μm; Millipore, Eschborn, Germany) and kept at –20°C. DNA was extracted from the five filters using the UltraClean Soil DNA Isolation Kit (MoBio, Solana, CA, USA) according to manufacturer's instructions. Bacterial 16S rRNA genes were PCR-amplified with the primers 27F and 1492R (Lane, 1991) as described before (Perner *et al*., 2009) but using only 10 cycles. For each sample three separate PCRs were performed, and the PCR amplicons were further divided into three aliquots. The first PCR aliquot was sequenced in the first sequencing run. The second and third PCR aliquots were sequenced in the second sequencing run and subsamples 1C2 and 1D2 were re-sequenced in a third sequencing run and named 1C4 and 1D4 respectively (for nomenclature of samples, see Table S1).

High-throughput sequencing of 16S rRNA genes

Bacterial tag-encoded FLX amplicon pyrosequencing was performed as described previously (Dowd *et al*., 2008a,b). Initial generation of the sequencing library utilized a PCR amplification with Hot Start Plus DNA polymerase (Qiagen, Valencia, CA, USA) and fusion primers that include both the 'tag' sequence and the adapter. For bacterial library construction, the primers were Gray28F 5′TTTGATCNTGGCTCAG (modified from Frias-Lopez *et al*., 2002) and Gray519r 5′GTNTTACNGCGGCKGCTG (modified from Manefield *et al*., 2002). All reactions used template with a concentration of 100 ng μl^{-1} and employed the following thermal profile: 1 cycle of 95°C for 5 min, 20 cycles of 95°C 30 s, 54°C for 40 s, 72°C for 1 min, 1 cycle of 72°C for 10 min. A secondary PCR

was performed for tag-encoded FLX amplicon pyrosequencing at the Research and Testing Laboratory (RTL; Lubbock, TX, USA) on a Roche 454 FLX instrument (454 Life Science, Branford, CT, USA) with Titanium reagents, following manufacture protocols.

Data analyses

The analysis was performed by combining different programs from the *Quantitative insights into microbial ecology* (Qiime) pipeline (Caporaso *et al*., 2010a), version 1.4.0, which provides methods for quality filtering of reads, efficient operational taxonomic unit (OTU) picking, taxonomy assignment and analysis of α- and β-diversity. First, all samples were denoised using AmpliconNoise 1.24 (Quince *et al*., 2011). This procedure allows for the reduction of the sequencing artefacts related to the PCR amplification and the pyrosequencing reactions. Additionally, it allows for the identification and removal of chimeric sequences. Pyrosequencing yielded 428 785 raw reads of length in the range between 32 bp and 844 bp (on average 367 bp, with a median length of 409 bp). Sequences were trimmed to at most 400 bp from the 5′ end, according to the quality scores. After denoising there were 302 280 sequence reads left, with a length ranging from 204 bp to 400 bp (average length: 394 bp, median length: 400 bp). Sequences were clustered *de novo* into OTUs using uclust (Edgar, 2010) (version 1.2.22) with a 97% similarity threshold. A single representative sequence for each OTU was then extracted and used in subsequent steps. The total number of OTUs picked in the raw data set was 13 640, while in the denoised data set the number of OTUs was 4796. The sharp decrease is expected and consistent with the finding in Wang and colleagues (2007). The accuracy in the estimation of the correct number of OTUs is increased by the denoising procedure (Reeder and Knight, 2009). All further analyses were performed using the denoised reads. Alpha rarefactions were used to investigate intra-sample variability. A phylogenetic tree relating to the OTUs was constructed as follows. A template-based multiple sequence alignment (MSA) of the set of representative sequences was prepared using PyNAST (Caporaso *et al*., 2010b) (version 1.1). The *GreenGenes core set* alignment, from the GreenGenes ribosomal database (DeSantis *et al*., 2006), provided with Qiime 1.4 was used as template. The alignment of the representative sequence set was filtered to remove gaps and hypervariable positions using the GreenGenes lane mask. From the resulting filtered MSA, an approximate maximum-likelihood phylogenetic tree was constructed using FastTree (Price *et al*., 2010) (version 2.1.3). The resulting tree was used for the calculation of the unweighted and normalized weighted UniFrac distances (Lozupone and Knight, 2005). β-diversity analyses were performed by principal coordinates analysis (PCoA) applied to the UniFrac distance matrices. To analyse the support of the data, jackknifing replicates were generated by random subsampling and included in the beta analysis. The interquartile ranges of the coordinates obtained from the analysis of the jackknife replicates are visualized as ellipsoids in the PCoA plots. To assess if the differences among the samples observed in the PCoA plots are significant, Bonferroni-corrected *P*-values were calculated using the UniFrac unweighted and normalized weighted significance tests as well as the *P*-test (Martin, 2002) available through the FastUniFrac website (http://bmf.colorado.edu/fastunifrac/). Furthermore, the representative sequence set was used for taxonomical assignments based on BLAST alignments to the GreenGenes set clustered at 97% similarity, version 4 February 2011. The maximum *E*-value to record an assignment was set to 0.001.

Data deposition

The sequence data have been deposited in the National Center for Biotechnology Information Sequence Read Archive (SRA) under the Accession Number SRP016119.

Acknowledgements

We thank the captain and crews of the German RV Maria S. Merian and ROV Kiel6000 (IFM-GEOMAR, Kiel) for helping us to obtain deep-sea vent samples. We thank Richard Seifert (University of Hamburg), Harald Strauss (Westfälische Wilhelms-Universität Münster, Germany) and Dieter Garbe-Schönberg (Christian-Albrechts-Universität, Kiel, Germany) for supplying hydrogen and methane (*ex situ*), sulfide as well as temperature and magnesium concentrations respectively. The work was supported by grants from the priority program 1144 'From Mantle to Ocean: Energy-, Material- and Life-Cycles at Spreading Axes' of the German Science Foundation (DFG). This is Publication No. 69.

References

Brazelton, W., Ludwig, K., Sogin, M., Andreishcheva, E., Kelley, D., Shen, C.-C., *et al*. (2010) Archaea and bacteria with surprising microdiversity show shifts in dominance over 1,000-year time scales in hydrothermal chimney. *Proc Natl Acad Sci USA* **107:** 1612–1617.

Campbell, B.J., Engel, A.S., Porter, M.L., and Takai, K. (2006) The versatile ε-proteobacteria: key players in sulphidic habitats. *Nat Rev Microbiol* **4:** 458–468.

Caporaso, J.G., Kuczynski, J., Stombaugh, J., Bittinger, K., Bushman, F.D., Costello, E.K., *et al*. (2010a) QIIME allows analysis of high-throughput community sequencing data. *Nat Methods* **7:** 335–336.

Caporaso, J.G., Bittinger, K., Bushman, F.D., DeSantis, T.Z., Andersen, G.L., and Knight, R. (2010b) PyNAST: a flexible tool for aligning sequences to a template alignment. *Bioinformatics* **26:** 266–267.

Carpenter, J.H. (1965) The Chesapeake Bay Institute technique for the Winkler dissolved oxygen method. *Limnol Oceanogr* **10:** 141–143.

Cline, J. (1969) Spectrophotometric determination of hydrogen sulfide in natural waters. *Limnol Oceanogr* **14:** 454–458.

Davis, R.E., and Moyer, C.L. (2008) Extreme spatial and temporal variability of hydrothermal microbial mat communities along the Mariana Island Arc and southern Mariana back-arc system. *J Geophys Res* **113:** B08S15.

DeLong, E.F., Preston, C.M., Mincer, T., Rich, V., Hallam, S.J., and Frigaard, N.U. (2006) Community genomics among stratified microbial assemblages in the ocean's interior. *Science* **311:** 496–503.

DeSantis, T.Z., Hugenholtz, P., Larsen, N., Rojas, M., Brodie, E.L., Keller, K., *et al*. (2006) Greengenes, a chimera-checked 16S rRNA gene database and workbench compatible with ARB. *Appl Environ Microbiol* **72:** 5069–5072.

Dowd, S.E., Callaway, T.R., Wolcott, R.D., Sun, Y., McKeehan, T., Hagevoort, R.G., and Edrington, T.S. (2008a) Evaluation of the bacterial diversity in the feces of cattle using 16S rDNA bacterial tag-encoded FLX amplicon pyrosequencing (bTEFAP). *BMC Microbiol* **8:** 125.

Dowd, S.E., Sun, Y., Wolcott, R.D., Domingo, A., and Carroll, J.A. (2008b) Bacterial tag-encoded FLX amplicon pyrosequencing (bTEFAP) for microbiome studies: bacterial diversity in the ileum of newly weaned Salmonella-infected pigs. *Foodborne Pathog Dis* **5:** 459–472.

Edgar, R. (2010) Search and clustering orders of magnitude faster than BLAST. *Bioinformatics* **26:** 2460–2461.

Flores, G.E., Campbell, J.H., Kirshtein, J.D., Meneghin, J., Podar, M., Steinberg, J.I., *et al*. (2011) Microbial community structure of hydrothermal deposits from geochemically different vent fields along the Mid-Atlantic Ridge. *Environ Microbiol* **13:** 2158–2171.

Flores, G.E., Shakya, M., Meneghin, J., Yang, Z.K., Seewald, J.S., Geoff Wheat, C., *et al*. (2012) Inter-field variability in the microbial communities of hydrothermal vent deposits from a back-arc basin. *Geobiology* **10:** 333–346.

Frias-Lopez, J., Zerkle, A.L., Bonheyo, G.T., and Fouke, B.W. (2002) Partitioning of bacterial communities between seawater and healthy, black band diseased, and dead coral surfaces. *Appl Environ Microbiol* **68:** 2214–2228.

Gonzalesz, J.M., and Whitman, W.B. (2006) *Oceanospirillum* and related genera. In *The Prokaryotes*. Dworkin, M., Falkow, S., Rosenberg, E., Schleifer, K.-H., and Stackebrandt, E. (eds). New York, NY, USA: Springer-Verlag, pp. 887–915.

Grote, J., Schott, T., Bruckner, C.G., Glockner, F.O., Jost, G., Teeling, H., *et al*. (2012) Genome and physiology of a model Epsilonproteobacterium responsible for sulfide detoxification in marine oxygen depletion zones. *Proc Natl Acad Sci USA* **109:** 506–510.

Huber, J.A., Mark Welch, D.B., Morrison, H.G., Huse, S.M., Neal, P.R., Butterfield, D.A., and Sogin, M.L. (2007) Microbial population structures in the deep marine biosphere. *Science* **318:** 97–100.

Huber, J.A., Cantin, H.V., Huse, S.M., Welch, D.B.M., Sogin, M.L., and Butterfield, D.A. (2010) Isolated communities of *Epsilonproteobacteria* in hydrothermal vent fluids of the Mariana Arc seamounts. *FEMS Microbiol Ecol* **73:** 538–549.

Lane, D.J. (1991) 16S/23S rRNA sequencing. In *Nucleic Acid Techniques in Bacterial Systematics*. Stackebrandt, E., and Goodfellow, M. (eds). Chichester, UK: John Wiley & Sons, pp. 115–175.

LeBris, N., Govenar, B., Le Gall, C., and Fisher, C.R. (2006) Variability of physico-chemical conditions in 9°50′N EPR diffuse flow vent habitats. *Mar Chem* **98:** 167–182.

Lozupone, C., and Knight, R. (2005) UniFrac: a new phylogenetic method for comparing microbial communities. *Appl Environ Microbiol* **71:** 8228–8235.

McCollom, T.M. (2007) Geochemical constraints on source of metabolic energy for chemolithoautotrophy in ultramafic-hosted deep-sea hydrothermal systems. *Astrobiology* **7:** 933–950.

Manefield, M., Whiteley, A.S., Griffiths, R.I., and Bailey, M.J. (2002) RNA stable isotope probing, a novel means of linking microbial community function to phylogeny. *Appl Environ Microbiol* **68:** 5367–5373.

Martin, A.P. (2002) Phylogenetic approaches for describing and comparing the diversity of microbial communities. *Appl Environ Microbiol* **68:** 3673–3682.

Nakagawa, S., Takai, K., Inagaki, F., Hirayama, H., Nunoura, T., Horikoshi, K., and Sako, Y. (2005) Distribution, phylogenetic diversity and physiological characteristics of epsilon-*Proteobacteria* in a deep-sea hydrothermal field. *Environ Microbiol* **7:** 1619–1632.

Nakagawa, S., Takaki, Y., Shimamura, S., Reysenbach, A.L., Takai, K., and Horikoshi, K. (2007) Deep-sea vent ε-proteobacterial genomes provide insights into emergence of pathogens. *Proc Natl Acad Sci USA* **104:** 12146–12150.

Nanoura, T., and Takai, K. (2009) Comparison of microbial communities associated with phase-separation-induced hydrothermal fuids at the Yonaguni Knoll IV hydrothermal field, the Southern Okinawa Trough. *FEMS Microbiol Ecol* **67:** 351–370.

Perner, M., Kuever, J., Seifert, R., Pape, T., Koschinsky, A., Schmidt, K., *et al*. (2007) The influence of ultramafic rocks on microbial communities at the Logatchev hydrothermal field, located 15°N on the Mid-Atlantic Ridge. *FEMS Microbiol Ecol* **61:** 97–109.

Perner, M., Bach, W., Hentscher, M., Koschinsky, A., Garbe-Schönberg, D., Streit, W.R., and Strauss, H. (2009) Short-term microbial and physico-chemical variability in low-temperature hydrothermal fluids near 5°S on the Mid-Atlantic Ridge. *Environ Microbiol* **11:** 2526–2541.

Perner, M., Petersen, J.M., Zielinski, F., Gennerich, H.-H., and Seifert, R. (2010) Geochemical constraints on the diversity and activity of H_2-oxidizing microorganisms in diffuse hydrothermal fluids from a basalt- and an ultramafic-hosted vent. *FEMS Microbiol Ecol* **74:** 55–71.

Perner, M., Hentscher, M., Rychlik, N., Seifert, R., Strauss, H., and Bach, W. (2011) Driving forces behind the biotope structures in the low-temperature venting at 5°S and 9°S MAR. *Environ Microbiol Rep* **3:** 727–737.

Price, M.N., Dehal, P.S., and Arkin, A.P. (2010) FastTree 2-approximately maximum-likelihood trees for large alignments. *PLoS ONE* **5:** e9490.

Quince, C., Lanzen, A., Davenport, R.J., and Turnbaugh, P.J. (2011) Removing noise from pyrosequenced amplicons. *BMC Bioinformatics* **12:** 38.

Reeder, J., and Knight, R. (2009) The 'rare biosphere': a reality check. *Nat Methods* **6:** 636–637.

Rocap, G., Larimer, F.W., Lamerdin, J., Malfatti, S., Chain, P., Ahlgren, N.A., *et al*. (2003) Genome divergence in two *Prochlorococcus* ecotypes reflects oceanic niche differentiation. *Nature* **424:** 1042–1047.

Rogers, K.L., Amend, J.P., and Gurrieri, S. (2007) Temporal changes in fluid chemistry and energy profiles in the Vulcano Island hydrothermal system. *Astrobiology* **7:** 905–932.

Sogin, M.L., Morrison, H.G., Huber, J.A., Welch, D.M., Huse, S.M., Neal, P.R., *et al*. (2006) Microbial diversity in the

deep sea and the underexplored 'rare biosphere'. *Proc Natl Acad Sci USA* **103:** 12115–12120.

Sunamura, M., Higashi, Y., Miyako, C., Ishibashi, J., and Maruyama, A. (2004) Two bacteria phylotypes are predominant in the Suiyo seamount hydrothermal plume. *Appl Environ Microbiol* **70:** 1190–1198.

Wang, Q., Garrity, G.M., Tiedje, J.M., and Cole, J.R. (2007) Naive bayesian classifier for rapid assignment of rRNA sequences into the new bacterial taxonomy. *Appl Environ Microbiol* **73:** 5261–5267.

Wankel, S.D., Germanovich, L.N., Lilley, M.D., Genc, G., DiPerna, C.J., Bradley, A.S., *et al*. (2011) Geochemical flux and metabolic activity associated with the hydrothermal subsurface. *Nat Geosci* **4:** 461–468.

Zielinski, F..U., Gennerich, H.H., Borowski, C., Wenzhöfer, F., and Dubilier, N. (2011) *In situ* measurements of hydrogen sulfide, oxygen, and temperature in diffuse fluids of an ultramafic-hosted hydrothermal vent field (Logatchev, 14°45′N, Mid-Atlantic Ridge): implications for chemosymbiotic bathymodiolin mussels. *G-cubed* **12:** Q0AE04.

Supporting information

Additional Supporting Information may be found in the online version of this article:

Fig. S1. Jackknife analysis of Irina II environment clusters using 100 permutations. Calculations were performed using unweighted (A) and weighted normalized (B) UniFrac algorithms. The inner nodes are coloured as follows: red for 75–100% support, yellow for 50–75%, green for 25–50%, blue for $< 25\%$ support. For subsample nomenclature, see Table S1.

Fig. S2. (A) Unweighted and (B) weighted normalized UniFrac algorithms were used for PCoA with subsamples from Irina II in the Logatchev and clustered according to the sequencing runs. Sequencing run 1 is colour-coded in red, sequencing run 2 in blue and sequencing run 3 in orange. The first three principal coordinates are plotted, and the axes are scaled according to the percentage variation explained by the corresponding coordinate.

Fig. S3. Cell counts in the five samples.

Fig. S4. Shannon diversity indices calculated from a set of rarefactions of the five samples.

Table S1. Nomenclature of the subsamples from the different sites segregated according to the PCR and the sequencing run.